



Low-Temperature Properties of the Dense Kondo System $\text{Ce}_{0.5}\text{La}_{0.5}\text{B}_6$

Shintaro NAKAMURA, Osamu SUZUKI, Terutaka GOTO, Shinichi SAKATSUME¹,
Takeshi MATSUMURA² and Satoru KUNII²

Graduate School of Science and Technology, Niigata University, Niigata 950-21

¹*Center for Low Temperature Science, Tohoku University, Sendai 980-77*

²*Department of Physics, Tohoku University, Sendai 980-77*

(Received October 25, 1996)

Low-temperature specific heat and electric resistivity of the dense Kondo compound $\text{Ce}_{0.5}\text{La}_{0.5}\text{B}_6$ have been measured. The specific heat for $H = 0$ shows a broad peak at around 0.9 K corresponding to the Kondo effect. No indication of magnetic or quadrupolar phase transition is observed down to 100 mK for $H = 0$. Very large specific heat coefficients of $\gamma = 1.8 \text{ J/K}^2 \text{ mol}$ and $\beta = 2.9 \text{ J/K}^4 \text{ mol}$ for $H = 0$ indicate the Kondo singlet ground state without long-range ordering.

KEYWORDS: dense Kondo effect, specific heat, magnetic phase diagram, quadrupolar ordering, $\text{Ce}_{0.5}\text{La}_{0.5}\text{B}_6$, electric resistivity

CeB_6 and its solid solutions of $\text{Ce}_x\text{La}_{1-x}\text{B}_6$ are well known as a Kondo system with a cubic CaB_6 -type crystal structure. The Kondo temperature of the $\text{Ce}_x\text{La}_{1-x}\text{B}_6$ system is estimated to be nearly 1 K, and depends slightly on Ce concentration.¹⁾ The trivalent Ce ion in the $4f^1$ configuration results in a $^2F_{5/2}$ ground state, which is further split by a cubic crystalline electric field (CEF) into a Γ_8 ground state and a Γ_7 excited one. Because of the large CEF splitting ($\Delta \sim 540 \text{ K}$) the low-temperature properties of $\text{Ce}_x\text{La}_{1-x}\text{B}_6$ are mainly governed by the Γ_8 quartet which has both magnetic and electric quadrupolar moments.²⁾

The diluted $\text{Ce}_x\text{La}_{1-x}\text{B}_6$ system has been investigated as the typical impurity Kondo system which has the orbitally degenerate ground state of Γ_8 . In diluted $\text{Ce}_x\text{La}_{1-x}\text{B}_6$ both the magnetic susceptibility and the elastic constant C_{44} show a crossover from the Curie behavior above $T_K = 1 \text{ K}$ to the temperature-independent behavior, due to the quenching of the magnetic and electric quadrupolar moments below T_K .^{3,4)} On the other hand, as a result of the coexistence of the intersite magnetic and quadrupolar interactions of the RKKY mechanism, pure CeB_6 shows a characteristic magnetic phase diagram. CeB_6 undergoes phase transitions from a paramagnetic phase *I* to an antiferroquadrupolar phase *II* at $T_Q = 3.3 \text{ K}$ and further to an antiferromagnetic phase *III* at $T_N = 2.3 \text{ K}$ in zero field.³⁾ Up to now the characteristic antiferroquadrupolar phase *II* of CeB_6 has attracted much attention.⁵⁻⁹⁾

Recently, the magnetic phase diagram of $\text{Ce}_{0.5}\text{La}_{0.5}\text{B}_6$ was reported.¹⁰⁾ No long-range ordering is developed under fields lower than $H_c = 17 \text{ kOe}$, and an antiferromagnetic phase *III* or an antiferroquadrupolar phase *II* is induced in magnetic fields higher than H_c . In the intermediate-concentration system $\text{Ce}_{0.5}\text{La}_{0.5}\text{B}_6$, the Kondo effect is in competition with intersite interactions. The Kondo effect must be dominant to realize the non

magnetic ground state in low fields, and the intersite interactions provide the long-range ordering in high fields. Although $\text{Ce}_{0.5}\text{La}_{0.5}\text{B}_6$ is an attractive system for studying the competition between the Kondo effect and the intersite interactions, low-temperature properties have not been well studied. In this paper, we present the low-temperature specific heat and electric resistivity of $\text{Ce}_{0.5}\text{La}_{0.5}\text{B}_6$.

The single crystal of $\text{Ce}_{0.5}\text{La}_{0.5}\text{B}_6$ was grown by the floating zone method. We prepared two samples of $\text{Ce}_{0.5}\text{La}_{0.5}\text{B}_6$: one 162.7 mg in weight for the specific heat measurement and the other a rectangle of $0.265 \times 0.650 \times 8 \text{ mm}^3$ for the electric resistivity measurement. Those samples were cut from the same ingot which was used for the ultrasonic measurements in ref. 10. The specific heat measurements were performed by the thermal relaxation method for temperatures of 170~700 mK in a ^3He - ^4He dilution refrigerator. For high temperatures above 700 mK we employed the adiabatic method, using a ^3He evaporating refrigerator. We used a RuO_2 thermometer which had been calibrated in magnetic fields in advance. The resistivity measurement was by the 4-terminal DC method, using ^3He and dilution refrigerators. We glued a small sintered silver sponge onto the sample and immersed the sample in liquid ^3He or ^3He - ^4He mixture directly.

In Fig. 1 we show the magnetic phase diagram of $\text{Ce}_{0.5}\text{La}_{0.5}\text{B}_6$ in the H - T plane. The closed circles indicate the experimental results of ultrasonic measurements.¹⁰⁾ The open circles and triangles indicate the transition points obtained by the specific heat and resistivity measurements which are described in detail as follows. In Fig. 2 we show the temperature dependence of the specific heat of $\text{Ce}_{0.5}\text{La}_{0.5}\text{B}_6$ under several fields applied along the $[001]$ axis. The specific heat for $H = 0$ in Fig. 2 shows a broad peak at around 0.9 K which corresponds to the formation of the non ordered Kondo singlet

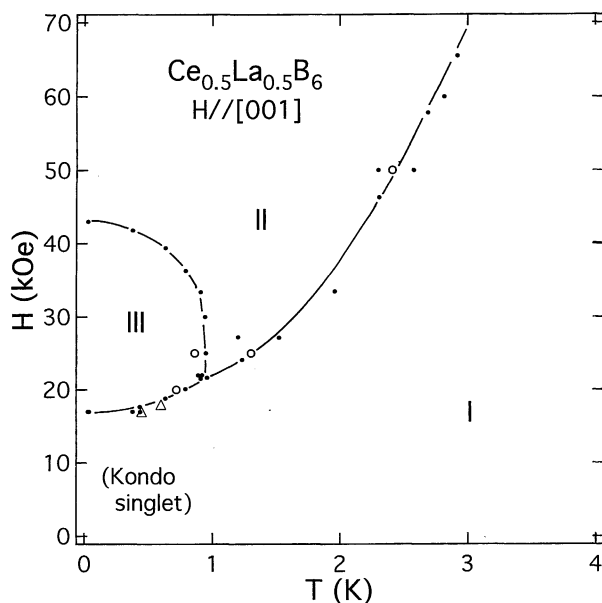


Fig. 1. The magnetic phase diagram of $\text{Ce}_{0.5}\text{La}_{0.5}\text{B}_6$. The field is applied along the [001] axis. The closed circles indicate the results taken from ref. 10. The open circles and open triangles indicate the present results obtained by specific heat and resistivity measurements, respectively.

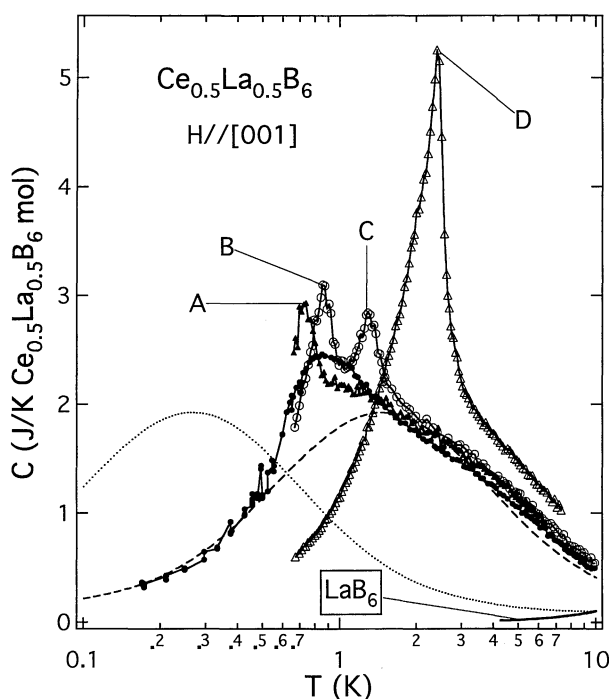


Fig. 2. The specific heat of $\text{Ce}_{0.5}\text{La}_{0.5}\text{B}_6$ for several fields. Here, the specific heat is obtained as the heat capacity per $\text{Ce}_{0.5}\text{La}_{0.5}\text{B}_6$ mole. The field is applied along the [001] axis. The closed circles, closed triangles, open circles and open triangles indicate the experimental results for $H = 0, 20 \text{ kOe}, 25 \text{ kOe}$ and 50 kOe , respectively. The dotted and broken lines correspond to the results of the renormalization group calculation for the Kondo temperatures $T_K = 1 \text{ K}$ and $T_K = 5.5 \text{ K}$, respectively.¹⁴⁾ The solid line indicates the specific heat of LaB_6 .

ground state. A similar broad peak due to the Kondo effect has been observed in the impurity Kondo system $\text{Ce}_x\text{La}_{1-x}\text{B}_6$ ($x = 0.0132$).¹¹⁾

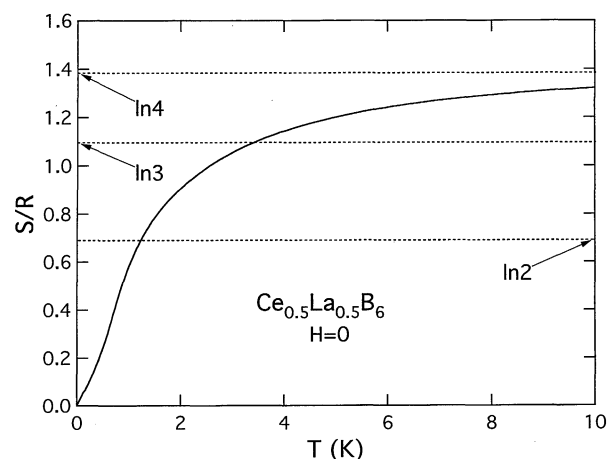


Fig. 3. The low-temperature dependence of the entropy of $\text{Ce}_{0.5}\text{La}_{0.5}\text{B}_6$ for $H = 0$.

When the applied field suppresses the Kondo effect, the intersite interactions produce long-range ordering above $H_c = 17 \text{ kOe}$. As shown in Fig. 2, a sharp peak 'A', which indicates the phase III/phase I transition, appears at around 0.7 K for $H = 20 \text{ kOe}$. Similar sharp peaks 'B' and 'C' for $H = 25 \text{ kOe}$ correspond to the phase III/phase II and phase II/phase I transitions, respectively. In the field of 50 kOe the specific heat of $\text{Ce}_{0.5}\text{La}_{0.5}\text{B}_6$ shows a λ -type peak 'D'. These phase transition points are plotted in Fig. 1 using open circles. The present results are consistent with the magnetic phase diagram obtained by ultrasonic measurements.¹⁰⁾

The temperature dependence of the entropy of $\text{Ce}_{0.5}\text{La}_{0.5}\text{B}_6$ for $H = 0$ is presented in Fig. 3. For calculation, we extrapolated the heat capacity of $\text{Ce}_{0.5}\text{La}_{0.5}\text{B}_6$ as the linear function of T down to 0 K and subtracted the heat capacity of LaB_6 from that of $\text{Ce}_{0.5}\text{La}_{0.5}\text{B}_6$ as the phonon contribution. The entropy reaches nearly $\ln 4$ at 10 K . This means that the large specific heat of $\text{Ce}_{0.5}\text{La}_{0.5}\text{B}_6$ is ascribed to the degrees of freedom of the Γ_8 quartet of the localized $4f$ electrons. We cannot find any indication of the phase transition of $\text{Ce}_{0.5}\text{La}_{0.5}\text{B}_6$ from the smooth increase of entropy seen in Fig. 3. On the contrary, in the more concentrated systems CeB_6 and $\text{Ce}_{0.75}\text{La}_{0.25}\text{B}_6$, clear anomalies of the entropy are observed at around $S/R = \ln 2$, associated with the antiferromagnetic ordering at T_N .¹²⁾

Next we compare the experimental result for $H = 0$ with the theoretical ones based on the Coqblin-Schrieffer model of a single impurity.¹³⁾ The numerical calculation was performed using the renormalization group method.¹⁴⁾ In CeB_6 , an increase of the Γ_8 - Γ_7 transition energy was observed in the Raman scattering for decrease of T from 20 K to 4 K .²⁾ This increase of the transition energy was interpreted in terms of a splitting of the Γ_8 state. The specific heat calculation for the diluted system $\text{Ce}_x\text{La}_{1-x}\text{B}_6$ ($x = 0.0132$) based on the split Γ_8 state model has also been performed.¹¹⁾ However, ultrasonic experiment gave no evidence of a splitting of the Γ_8 state in $\text{Ce}_x\text{La}_{1-x}\text{B}_6$.¹⁵⁻¹⁸⁾ For $\text{Ce}_{0.5}\text{La}_{0.5}\text{B}_6$, considerable decrease of the elastic constant C_{44} and increase of the ultrasonic attenuation of the C_{44} mode have been

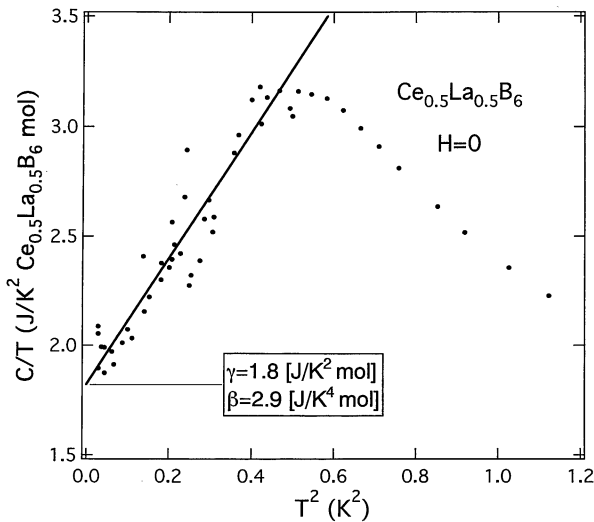


Fig. 4. The low-temperature specific heat of $\text{Ce}_{0.5}\text{La}_{0.5}\text{B}_6$ for $H = 0$ on an expanded scale. Here, the specific heat is obtained as the heat capacity per $\text{Ce}_{0.5}\text{La}_{0.5}\text{B}_6$ mole. The solid line is fitted for the temperatures of $0.17\text{ K} < T < 0.60\text{ K}$ using $C/T = \gamma + \beta T^2$.

observed at temperatures lower than 1 K .⁴⁾ Such behaviors are difficult to explain in terms of the split Γ_8 state. Therefore, at the present time, we assume the four fold degenerated Γ_8 ground state of $\text{Ce}_{0.5}\text{La}_{0.5}\text{B}_6$ in the calculations. The dotted line in Fig. 2 shows the calculated result for $T_K = 1\text{ K}$ and the broken line, for $T_K = 5.5\text{ K}$. The excited Γ_7 level is neglected in the present calculation. The calculated results for $T_K = 1\text{ K}$ show a broad peak at around 0.27 K ($\sim T_K/4$), and are in poor agreement with the experimental data. When we choose the Kondo temperature as $T_K = 5.5\text{ K}$, the calculated results of the broken line well reproduce the experimental data at temperatures higher than 2 K . However, $T_K = 5.5\text{ K}$ of this calculation is much higher than the experimental value of $T_K = 1\text{ K}$ in the $\text{Ce}_x\text{La}_{1-x}\text{B}_6$ system.^{1, 19)} Moreover, a clear discrepancy between the experimental and the calculated results for $T_K = 5.5\text{ K}$ is found below 2 K . These disagreements may be ascribed to the fluctuation effect due to the intersite interactions among the magnetic and quadrupolar moments of the $4f$ electrons. In spite of these disagreements, the Coqblin-Schrieffer model of single impurity can be used to explain the temperature dependence of the specific heat of $\text{Ce}_{0.5}\text{La}_{0.5}\text{B}_6$ at temperatures higher than 2 K . The intersite interactions among the $4f$ electrons, which are neglected in the impurity model, may result in the apparent increase of T_K and the rather sharp specific heat peak.

The zero field specific heat is presented in Fig. 4 as a function of T^2 on an expanded scale. The specific heat of $\text{Ce}_{0.5}\text{La}_{0.5}\text{B}_6$ roughly follows the $C/T = \gamma + \beta T^2$ law at low temperatures. The solid line in Fig. 4 is the fitted line. The specific heat coefficients $\gamma = 1.8\text{ J/K}^2\text{ mol}$ and $\beta = 2.9\text{ J/K}^4\text{ mol}$ of $\text{Ce}_{0.5}\text{La}_{0.5}\text{B}_6$ are obtained. The values of $\gamma = 0.25\text{ J/K}^2\text{ mol}$ and $\beta = 1.2\text{ J/K}^4\text{ mol}$ for CeB_6 and $\gamma = 0.3 \sim 0.4\text{ J/K}^2\text{ mol}$ and $\beta = 2.3\text{ J/K}^4\text{ mol}$ for $\text{Ce}_{0.75}\text{La}_{0.25}\text{B}_6$ have already been reported.¹²⁾ These coefficients are summarized in Table I. In $\text{Ce}_{0.5}\text{La}_{0.5}\text{B}_6$, the non magnetic ground state due to the Kondo effect

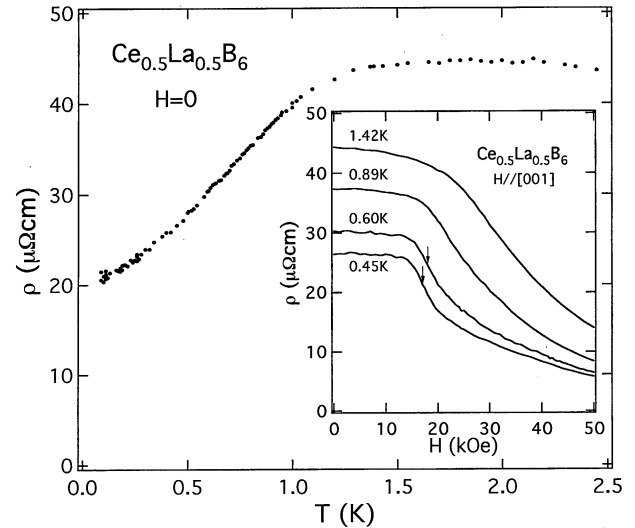


Fig. 5. The low-temperature electric resistivity of $\text{Ce}_{0.5}\text{La}_{0.5}\text{B}_6$ for $H = 0$. The magnetic resistivity at several temperatures are shown in the inset. Here, the current is directed along the $[110]$ axis. The field is applied along the $[001]$ axis. The phase transition points indicated by the arrows in the inset are presented in Fig. 1 as open triangles.

Table I. Low-temperature specific heat coefficients of the Kondo compounds $\text{Ce}_x\text{La}_{1-x}\text{B}_6$ for a formula of $C/T = \gamma + \beta T^2$.

sample	γ (J/K ² mol)	β (J/K ⁴ mol)
CeB_6 ^{a)}	0.25	1.2
$\text{Ce}_{0.75}\text{La}_{0.25}\text{B}_6$ ^{a)}	0.4~0.3	2.3
$\text{Ce}_{0.5}\text{La}_{0.5}\text{B}_6$	1.8	2.9

a) From ref. 12.

leads to very large specific heat coefficients at low temperatures, which are in sharp contrast to the relatively small coefficients in the antiferromagnetic ordered systems CeB_6 and $\text{Ce}_{0.75}\text{La}_{0.25}\text{B}_6$.

The electric resistivity of $\text{Ce}_{0.5}\text{La}_{0.5}\text{B}_6$ are presented in Fig. 5. The resistivity for $H = 0$ decreases with decreasing temperature below 1.5 K . However, no obvious anomaly indicating phase transition is observed down to 100 mK . The resistivity of $\text{Ce}_{0.5}\text{La}_{0.5}\text{B}_6$ at 100 mK is about $21\text{ }\mu\Omega\text{cm}$. This large residual resistivity is not mainly a result of the scattering by the spherical Coulomb potential of the randomly distributed Ce^{3+} and La^{3+} ions.¹⁹⁾ As shown in the inset of Fig. 5, the magnetoresistivity for $T = 0.60\text{ K}$ and 0.45 K show only weak field dependence in the fields lower than 17 kOe . However, the magnetoresistivity for $T = 0.60\text{ K}$ and 0.45 K show clear anomalies, corresponding to the phase I/phase III transition, which are indicated by arrows. The resistivity drastically decreases with development of the magnetic long-range ordering. This implies that the high residual resistivity in zero field is mainly ascribed to the Kondo effect in the non ordered state.

We have performed the low-temperature specific heat and electric resistivity measurements of $\text{Ce}_{0.5}\text{La}_{0.5}\text{B}_6$. The present results verify the magnetic phase diagram obtained by the previous ultrasonic measurements. The zero field specific heat of $\text{Ce}_{0.5}\text{La}_{0.5}\text{B}_6$ shows a broad

peak at around 0.9 K, which is a common characteristic of diluted Kondo systems. The Coqblin-Schrieffer model of a single impurity reproduces essential features of specific heat for $H = 0$ at temperatures higher than 2 K. The zero field specific heat of $\text{Ce}_{0.5}\text{La}_{0.5}\text{B}_6$ at low temperatures roughly follows the $C = \gamma T + \beta T^3$ law. The large specific heat coefficients $\gamma = 1.8 \text{ J/K}^2 \text{ mol}$ and $\beta = 2.9 \text{ J/K}^4 \text{ mol}$ indicate the non magnetic Kondo ground state. In applying the magnetic field, phase *I* of the non magnetic ground state of $\text{Ce}_{0.5}\text{La}_{0.5}\text{B}_6$ changes to the long-range ordered phase *II* or phase *III*. Low-temperature resistivity of $\text{Ce}_{0.5}\text{La}_{0.5}\text{B}_6$ for $H = 0$ is $21 \mu\Omega\text{cm}$ at 100 mK. This high residual resistivity is a result of the Kondo effect.

Acknowledgment

We are grateful to Dr. Y. Shimizu for providing the specific heat calculated, using the renormalization group method. This work was supported by a Grant-in-Aid from the Ministry of Education, Science and Culture. S. Nakamura wishes to acknowledge JSPS Fellowships for Japanese Junior Scientists for financial support.

-
- 1) N. Sato, S. Kunii, I. Oguro, T. Komatsubara and T. Kasuya: J. Phys. Soc. Jpn. **53** (1984) 3967.
 - 2) E. Zirngiebl, B. Hillebrands, S. Blumenröder, G. Güntherodt, M. Loewenhaupt, J. M. Carpenter, K. Winzer and Z. Fisk:

- Phys. Rev. B **30** (1984) 4052.
- 3) W. Felsch: Z. Phys. B **29** (1978) 211.
- 4) S. Nakamura, T. Goto, K. Morita, S. Sakatsume and S. Kunii: Physica B **206&207** (1995) 320.
- 5) J. M. Effantin, J. Rossat-Mignod, P. Burlet, H. Bartholin, S. Kunii and T. Kasuya: J. Magn. Magn. Mater. **47&48** (1985) 145.
- 6) M. Takigawa, H. Yasuoka, T. Tanaka and Y. Ishizawa: J. Phys. Soc. Jpn. **52** (1983) 728.
- 7) K. Hanzawa and T. Kasuya: J. Phys. Soc. Jpn. **53** (1984) 1809.
- 8) F. J. Ohkawa: J. Phys. Soc. Jpn. **54** (1985) 3909 and references therein.
- 9) G. Uimin, Y. Kuramoto and N. Fukushima: Solid State Commun. **97** (1996) 595.
- 10) S. Nakamura, T. Goto and S. Kunii: J. Phys. Soc. Jpn. **64** (1995) 3941.
- 11) H. Gruhl and K. Winzer: Solid State Commun. **57** (1986) 67.
- 12) T. Furuno, N. Sato, S. Kunii, T. Kasuya and W. Sasaki: J. Phys. Soc. Jpn. **54** (1985) 1899.
- 13) B. Coqblin and J. R. Schrieffer: Phys. Rev. **185** (1969) 847.
- 14) Y. Shimizu and O. Sakai: J. Phys. Soc. Jpn. **65** (1996) 2632.
- 15) B. Lüthi, S. Blumenröder, B. Hillebrands, E. Zirngiebl, G. Güntherodt and K. Winzer: Z. Phys. B **58** (1984) 31.
- 16) T. Goto, T. Suzuki, Y. Ohe, T. Fujimura and A. Tamaki: J. Magn. Magn. Mater. **76&77** (1988) 305.
- 17) S. Nakamura, T. Goto, S. Kunii, K. Iwashita and A. Tamaki: J. Phys. Soc. Jpn. **63** (1994) 623.
- 18) P. Lemmens, S. Ewert, P. Thalmeier, D. Lenz and K. Winzer: Z. Phys. B **76** (1989) 501.
- 19) N. Sato, A. Sumiyama, S. Kunii, H. Nagano and T. Kasuya: J. Phys. Soc. Jpn. **54** (1985) 1923.